



Comprehensive Assessment of Coronary Plaque Progression With Advanced Intravascular Imaging, Physiological Measures, and Wall Shear Stress: A Pilot Double-Blinded Randomized Controlled Clinical Trial of Nebivolol Versus Atenolol in Nonobstructive Coronary Artery Disease

Olivia Y. Hung, *Emory University*
David Molony, *Georgia Institute of Technology*
Michael T. Corban, *Emory University*
Emad Rasoul-Arzrumly, *Emory University*
Charles Maynard, *University of Washington*
Parham Eshtehardi, *Emory University*
Saurabh Dhawan, *Emory University*
Lucas Timmins, *Emory University*
[Marina Piccinelli](#), *Emory University*
Sung Gyun Ahn, *Emory University*

Only first 10 authors above; see publication for full author list.

Journal Title: Journal of the American Heart Association
Volume: Volume 5, Number 1
Publisher: American Heart Association: JAHA | 2016-01-01
Type of Work: Article | Final Publisher PDF
Publisher DOI: 10.1161/JAHA.115.002764
Permanent URL: <https://pid.emory.edu/ark:/25593/rqn5v>

Final published version: <http://dx.doi.org/10.1161/JAHA.115.002764>

Copyright information:

© 2016 The Authors. Published on behalf of the American Heart Association, Inc., by Wiley Blackwell.

This is an Open Access work distributed under the terms of the Creative Commons Attribution-NonCommercial 4.0 International License (<http://creativecommons.org/licenses/by-nc/4.0/>).



Comprehensive Assessment of Coronary Plaque Progression With Advanced Intravascular Imaging, Physiological Measures, and Wall Shear Stress: A Pilot Double-Blinded Randomized Controlled Clinical Trial of Nebivolol Versus Atenolol in Nonobstructive Coronary Artery Disease

Olivia Y. Hung, MD, PhD; David Molony, PhD; Michel T. Corban, MD; Emad Rasoul-Arzrumly, MD; Charles Maynard, PhD; Parham Eshtehardi, MD; Saurabh Dhawan, MD; Lucas H. Timmins, PhD; Marina Piccinelli, PhD; Sung Gyun Ahn, MD, PhD; Bill D. Gogas, MD, PhD; Michael C. McDaniel, MD; Arshed A. Quyyumi, MD; Don P. Giddens, PhD; Habib Samady, MD

Background—We hypothesized that nebivolol, a β -blocker with nitric oxide-mediated activity, compared with atenolol, a β -blocker without such activity, would decrease oxidative stress and improve the effects of endothelial dysfunction and wall shear stress (WSS), thereby reducing atherosclerosis progression and vulnerability in patients with nonobstructive coronary artery disease.

Methods and Results—In this pilot double-blinded randomized controlled trial, 24 patients treated for 1 year with nebivolol 10 mg versus atenolol 100 mg plus standard medical therapy underwent baseline and follow-up coronary angiography with assessments of inflammatory and oxidative stress biomarkers, microvascular function, endothelial function, and virtual histology intravascular ultrasound. WSS was calculated from computational fluid dynamics. Virtual histology intravascular ultrasound segments were assessed for vessel volumetrics and remodeling. There was a trend toward more low-WSS segments in the nebivolol cohort ($P=0.06$). Low-WSS regions were associated with greater plaque progression ($P<0.0001$) and constrictive remodeling ($P=0.04$); conversely, high-WSS segments demonstrated plaque regression and excessive expansive remodeling. Nebivolol patients had decreased lumen and vessel areas along with increased plaque area, resulting in more constrictive remodeling ($P=0.002$). There were no significant differences in biomarker levels, microvascular function, endothelial function, or number of thin-capped fibroatheromas per vessel. Importantly, after adjusting for β -blocker, low-WSS segments remained significantly associated with lumen loss and plaque progression.

Conclusion—Nebivolol, compared with atenolol, was associated with greater plaque progression and constrictive remodeling, likely driven by more low-WSS segments in the nebivolol arm. Both β -blockers had similar effects on oxidative stress, microvascular function, and endothelial function.

Clinical Trial Registration—URL: <https://clinicaltrials.gov/>. Unique identifier: NCT01230892. (*J Am Heart Assoc.* 2016;5:e002764 doi: 10.1161/JAHA.115.002764)

Key Words: coronary flow • coronary microvascular function • endothelial function • intravascular ultrasound • wall shear stress

Alterations in coronary wall shear stress (WSS) can interact with the endothelium to affect the distribution, progression, and pathophysiology of atherosclerosis,^{1–9} and

several studies have demonstrated the association between WSS magnitudes and plaque development.^{3–10} In particular, low WSS (<1.0 Pa) has been related to plaque

From the Division of Cardiology, Department of Medicine, Andreas Gruentzig Cardiovascular Center, Emory University School of Medicine, Atlanta, GA (O.Y.H., M.T.C., E.R.-A., P.E., S.D., L.H.T., S.G.A., B.D.G., M.C.M., A.A.O., H.S.); Division of Cardiology, Department of Internal Medicine, Yonsei University Wonju College of Medicine, Wonju, Republic of Korea (S.G.A.); Wallace H. Coulter Department of Biomedical Engineering, Georgia Institute of Technology and Emory University, Atlanta, GA (D.M., L.H.T., D.P.G.); Department of Health Services, University of Washington, Seattle, WA (C.M.); Department of Radiology and Imaging Sciences, Emory University, Atlanta, GA (M.P.).

An accompanying Video S1 is available at <http://jaha.ahajournals.org/content/5/1/e002764/suppl/DC1>

Correspondence to: Habib Samady, MD, FACC, FSCAI, Emory University School of Medicine, 1364 Clifton Road F622, Atlanta, GA 30322. E-mail: hsamady@emory.edu

Received October 21, 2015; accepted November 18, 2015.

© 2016 The Authors. Published on behalf of the American Heart Association, Inc., by Wiley Blackwell. This is an open access article under the terms of the Creative Commons Attribution-NonCommercial License, which permits use, distribution and reproduction in any medium, provided the original work is properly cited and is not used for commercial purposes.

progression,^{5–10} whereas high WSS (>2.5 Pa) has been associated with increased necrotic core area on virtual histology intravascular ultrasound (VH-IVUS), a marker of plaque vulnerability.^{3,4,9,10} The impact of valsartan and simvastatin on the proinflammatory effect of low WSS has been studied in the swine model¹¹; however, the effect of an endothelial protective pharmaceutical agent, such as nebivolol, on the interplay between WSS and the progression of human coronary atherosclerosis has not been investigated.

Nebivolol is a third-generation β_1 receptor–selective antagonist with nitric oxide–mediated vasodilatory effect approved by the US Food and Drug Administration for treatment of hypertension and in Europe for left ventricular systolic dysfunction. Previous studies have suggested that nebivolol decreases coronary microvascular resistance through an agonist effect on the endothelial β_3 receptor, which mediates nitric oxide– and endothelium-dependent vasorelaxation.^{12–16} Enhanced flow and nitric oxide availability may decrease vascular reactivity and lipid oxidation and prove beneficial in conditions such as atherosclerosis, in which oxidative stress leads to decreased endothelial nitric oxide synthase expression and nitric oxide bioavailability. Potential benefits from nebivolol therapy may be observed in measures of endothelial function, microvascular function, vascular remodeling, or epicardial plaque burden and composition.

Accordingly, we conducted a pilot double-blinded randomized controlled trial on the effect of 1 year of nebivolol versus atenolol therapy on the changes in the number of thin-capped fibroatheromas (TCFAs) per vessel and in coronary plaque volumetrics among different WSS categories in patients with nonobstructive coronary artery disease. We hypothesized that nebivolol, by decreasing oxidative stress and improving endothelial function, would favorably affect atherosclerosis progression compared with atenolol, a β -blocker without nitric oxide–mediated activity.

Methods

Participants and Study Design

This single-center double-blinded randomized trial (NCT01230892) enrolled patients with recurrent angina symptoms who presented to the cardiac catheterization laboratory at Emory University Hospital from 2010 to 2012 and were found to have coronary nonobstructive atherosclerotic lesions (<50% stenosis by angiography or <70% stenosis with fractional flow reserve >0.80). Patients provided written informed consent for participation in this study prior to the baseline cardiac catheterization and randomization.

Inclusion criteria included patients being on stable medical therapy, presentation of stable angina or non–ST-segment

elevation acute coronary syndrome, and coronary lesion in the proximal 60 mm of an epicardial vessel deemed significant enough by the operator to warrant further evaluation using physiology and VH-IVUS. Patients were excluded if they presented with cardiogenic shock, ejection fraction <30%, or significant hepatic, hematologic, or renal impairment; had a history of coronary artery bypass surgery or severe valvular heart disease; could not provide informed consent; or had any contraindication to β -blocker therapy. Anatomically, cases were excluded if there were lesions requiring revascularization or significant visual coronary collaterals.

After undergoing baseline coronary angiography with VH-IVUS and evaluation of coronary microvascular and endothelial function, patients were randomized (1:1) to nebivolol 10 mg daily (first week 5 mg daily) or atenolol 100 mg daily (first week 50 mg daily) for 1 year. Nebivolol 5 mg (Forest Laboratories) and atenolol 50 mg (AstraZeneca Pharmaceuticals) have equivalent efficacy for reducing blood pressure.¹⁷

The Investigational Drug Service at our institution performed simple randomization using the online program “Research Randomizer” to generate the randomization plan in blocks of 4; dispensed the blinded study medication (same tablet size, shape, and color, with the same bottles and labels); and maintained separate records using WebIDS, a fully Health Insurance Portability and Accountability Act–compliant system that maintains protocol and drug information, patient profiles, randomization assignments, inventory records, and dispensing and patient return information. Enrolled patients were treated for 12±3 months with the study drug plus standard medical therapy (aspirin, statin, and as needed sublingual nitroglycerin) followed by repeat coronary angiography with VH-IVUS and assessments of microvascular and endothelial function (Figure 1). Participants, care providers, and study investigators were blinded until after completion of the last follow-up visit.

The Emory University institutional review board approved the study, and there were no significant changes to the protocol after the trial commenced. The primary end point was the change in the number of TCFAs per vessel between baseline and follow-up. Secondary end points included inflammatory and oxidative stress biomarkers, endothelial function, microvascular function, static and serial arterial remodeling, and VH-IVUS plaque area and composition at baseline and 1-year follow-up.

Lipids and Biomarkers

Basic metabolic panel, complete blood count, fasting lipid panel, and C-reactive protein level were collected the day of angiography and measured by the hospital medical laboratory services. Samples for plasma glutathione and cystine measurements were collected immediately after obtaining vascu-

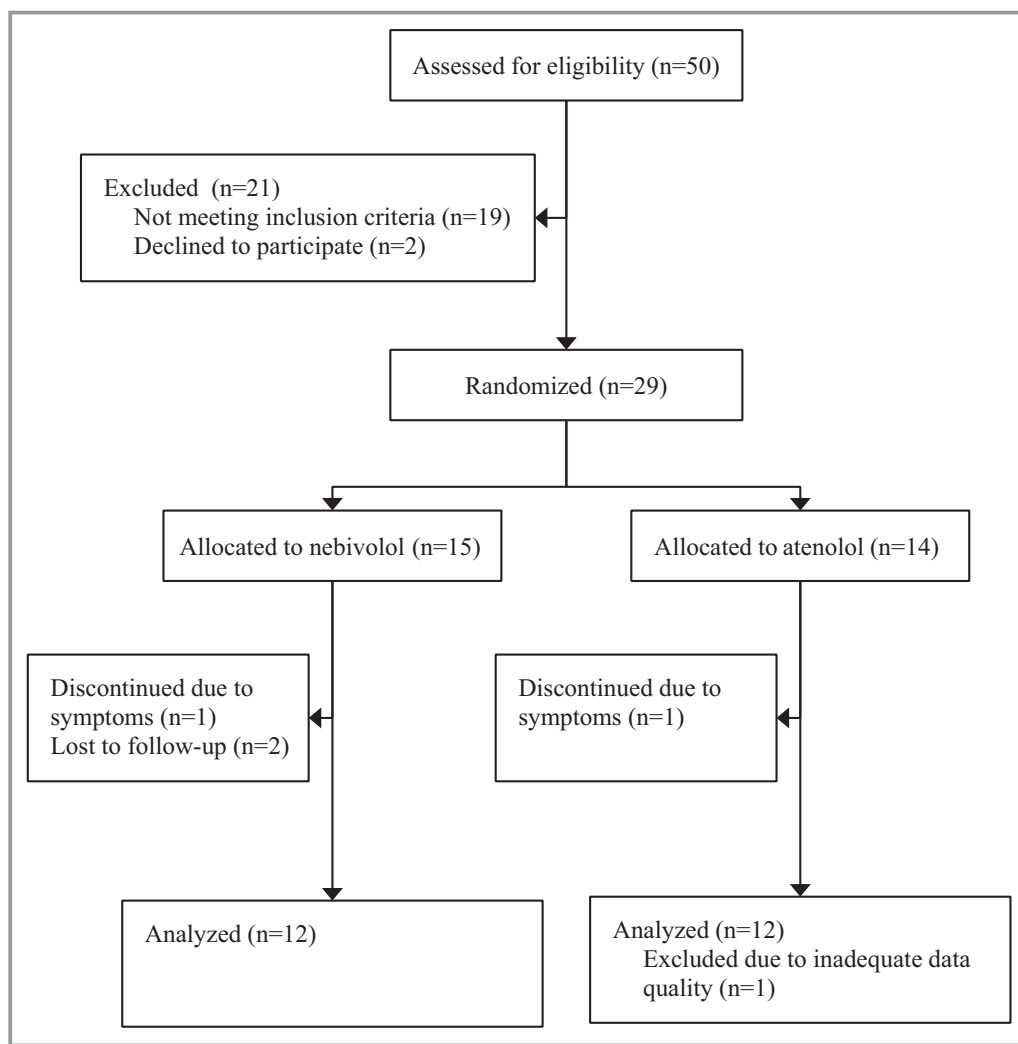


Figure 1. Study flowchart.

lar access in the cardiac catheterization laboratory, were frozen at -80°C , and were measured by the Emory University clinical biomarkers core laboratory. These samples have been shown to be stable under these conditions for 1 year.¹⁸

Cardiac Catheterization With Assessment of Endothelial and Microvascular Function

All β -blockers were withheld for ≥ 48 hours and long-acting nitrates were withheld for ≥ 24 hours prior to cardiac catheterization (both baseline and follow-up procedures). Procedures were performed in the morning after patients had fasted for at least 8 hours. Systolic and diastolic blood pressures and heart rate were measured prior to the start of the procedure. Patients underwent angiography in a biplane cardiac catheterization system (Toshiba America Medical Systems) using a standard 6F technique.

Pressure and velocity measurements were obtained using a 0.014-in pressure and Doppler flow velocity monitoring

guidewire (ComboWire: Volcano Corporation). For safety considerations, only the left coronary system was interrogated. The ComboWire was advanced to the guide catheter tip, at which the aortic pressure and guidewire pressures were equalized. Microvascular function was evaluated from pressure and velocity responses to intravenous adenosine infusion ($140 \mu\text{g}/\text{kg}$ per minute) for 3 minutes. At maximal hyperemia, fractional flow reserve was measured as the ratio of distal to aortic pressure, and hyperemic microvascular resistance was measured as the ratio of distal pressure to average peak flow velocity. Coronary flow velocity reserve was defined as the ratio of hyperemic to basal average peak flow velocity. Velocity measurements demonstrated good reproducibility, with a concordance correlation coefficient of 0.979 (95% CI 0.966–0.988).⁹

Endothelial function was assessed as the percentage change in coronary diameter and blood flow in response to intracoronary acetylcholine (off-label use) using Doppler flow velocity measurements and quantitative coronary angiography

(QAngio XA 7.3; Medis Medical Imaging Systems). Patients were first evaluated with 10^{-8} mol/L acetylcholine for safety prior to proceeding with 10^{-6} mol/L acetylcholine. Figure 2 demonstrates Doppler velocity envelopes prior to and during medication infusion in 1 patient at baseline and follow-up.

VH-IVUS Acquisition and Analysis

VH-IVUS acquisition was performed after administration of 200 μ g intracoronary nitroglycerin using phased-array 20 MHz Eagle Eye catheters and a s5 Imaging System (Volcano Corporation). Automated motorized pullback (0.5 mm/s) was performed, and VH-IVUS images were continuously acquired up to the guide catheter in the aorta (up to 60 mm of the proximal vessel). Angiography was used to record the catheter start position and its relationship to anatomic branching landmarks to aid with coregistration.

Offline analysis was performed at the Emory cardiovascular imaging and biomechanical core laboratory by experienced investigators who were blinded to the patients' clinical data according to the criteria of the American College of Cardiology Clinical Consensus document on IVUS,^{19,20} using VIAS

version 3.0 (Volcano Corporation) and echoPlaque 4.0.27 (INDEC Medical Systems). Measurements of the external elastic membrane (EEM), plaque, and lumen cross-sectional areas were performed for every recorded VH-IVUS cross-section (0.5-mm thickness), defined as a segment in the current analysis. Plaque burden was calculated as plaque area divided by EEM area. Segments involving bifurcating branch points or precluding complete lumen or vessel wall planimetry were excluded from analysis. Intraobserver analysis demonstrated good reproducibility for plaque area (concordance correlation coefficient 0.968 [95% CI 0.965–0.971]).⁹

Different nomenclatures have been used to describe arterial remodeling patterns. We defined static remodeling as the ratio of lesion to reference EEM area, also known as the remodeling index. We also used *excessive expansive*, *compensatory*, and *constrictive* to describe 3 patterns of serial remodeling.¹⁹ For each segment, positive Δ EEM area was defined as positive remodeling, and negative Δ EEM area was defined as constrictive remodeling. Segments with positive remodeling were further subdivided as compensatory if the ratio of Δ EEM area to Δ plaque area was between 0.0 and 1.0 or as excessive expansive otherwise.

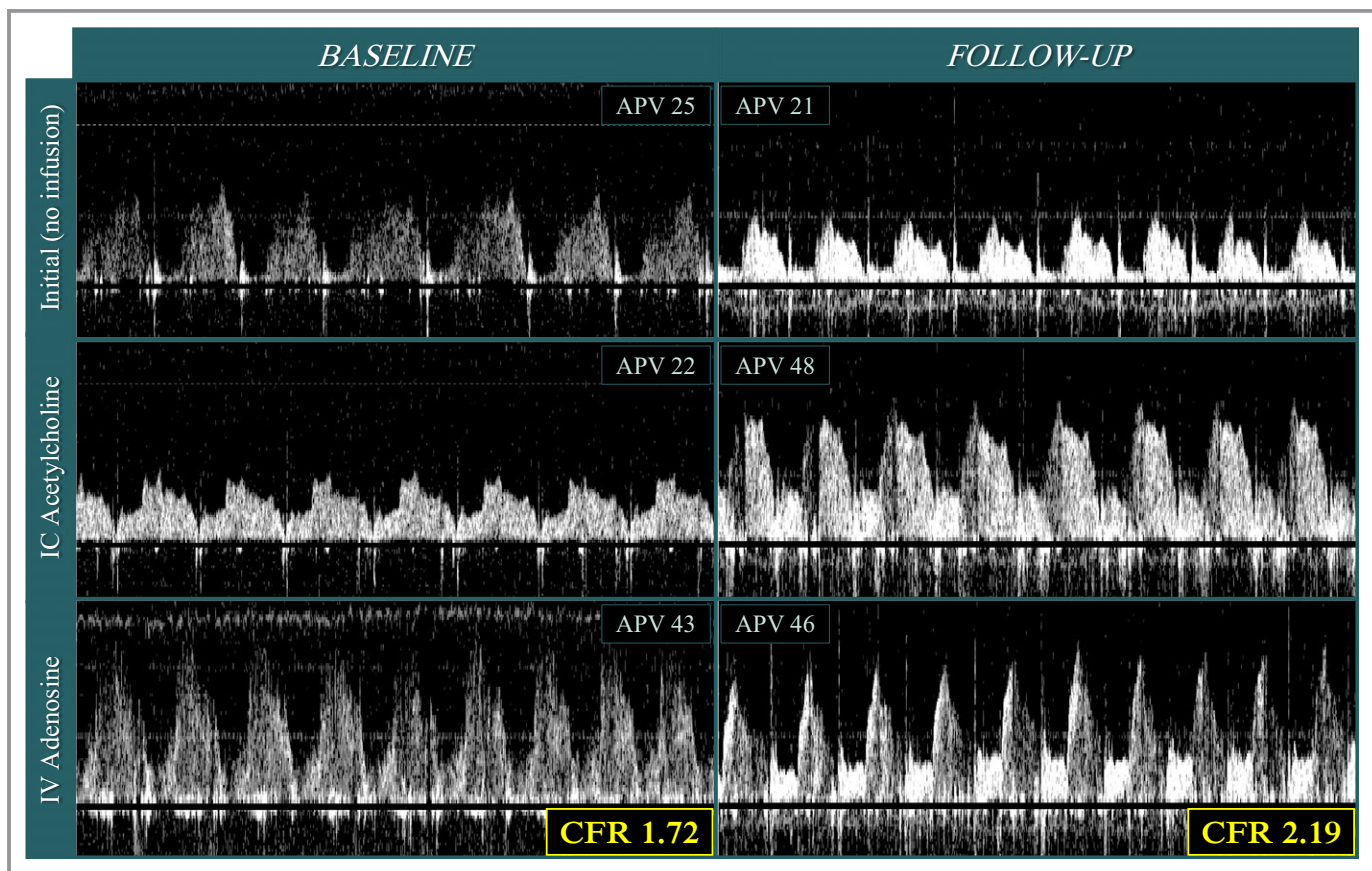


Figure 2. Doppler velocity waveforms obtained from a patient undergoing endothelial and microvascular function assessment at baseline and 1-year follow-up. APV indicates average peak velocity; CFR, coronary flow reserve; IC, intracoronary; IV, intravenous.

Finally, lesions were classified based on plaque composition as assessed by VH-IVUS (fibrous, fibrofatty, necrotic core, and dense calcium) for each segment.^{20,21} Fibroatheromas were defined as $\geq 40\%$ plaque burden and $\geq 10\%$ necrotic core; TCFAs were fibroatheromas with necrotic core abutting the lumen in at least 3 consecutive frames.

Computational Fluid Dynamics and Baseline WSS Analysis

WSS analysis methodology using the ANGUS method has been described previously.^{1,9} Briefly, the 3-dimensional path of the VH-IVUS catheter was determined using corresponding biplane angiographic projections acquired at the start of pullback. Each frame was rotated and aligned perpendicular to the catheter core to reconstruct the main artery of interest. Arterial branches were added based on information from angiography and VH-IVUS. Patient-specific pulsatile inlet boundary conditions were determined from Doppler wire-derived waveforms, and the outlets were assumed to be pressure-free. The reconstructed surface was meshed and imported into Fluent (ANSYS). After computing the pulsatile flow field in the region of interest, WSS was determined as a function of time in the cardiac cycle and spatial location around the lumen (Video S1, Figure 3) and then averaged over time and circumference at each cross-section for quantitative

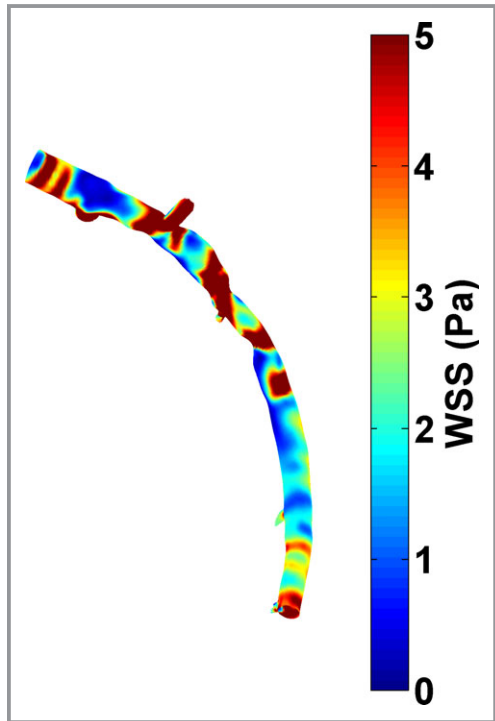


Figure 3. A patient-specific WSS profile of the left anterior descending coronary artery demonstrates areas of variable WSS magnitudes. WSS indicate wall shear stress.

analysis. Although WSS is a continuous and dynamic variable, based on previous cell culture and experimental and human data, WSS magnitudes were categorized as low (< 1.0 Pa), intermediate (≥ 1.0 and < 2.5 Pa), or high (≥ 2.5 Pa).^{3,9,22,23}

Statistical Analysis

Sample size was not determined strictly from effect sizes because the purpose of this pilot study was to generate data to power future clinical trials. It was estimated using previous comparative studies between nebivolol and atenolol on endothelial and microvascular function assuming a 0.05 significance level and 0.80 power value.^{13,15,16}

Continuous variables are described as mean \pm SD or median and interquartile range, as appropriate, and categorical variables are described as counts and proportions. For patient-level analyses, the chi-square statistic was used to compare categorical variables (eg, hypertension), and the 2-sample *t* test was used for continuous variables (eg, age). The differences between baseline and follow-up patient-level measures (eg, systolic blood pressure) were computed for each group, and the differences between the 2 groups were compared with the 2-sample *t* test.

Correlated error is introduced by the clustering of arterial segments within patients. To correct for this, *P* values were adjusted with linear regression for continuous outcomes (eg, Δ lumen area) and ordered logistic regression for categorical variables (eg, serial arterial remodeling). In both situations, the Huber White Sandwich Estimator was used to adjust the *P* values for correlated error.^{24,25} To further examine the association of WSS, drug, and change measures, mixed models with WSS and drug as predictor variables were run. Although there are many observations at the VH-IVUS segmental level, the effective sample size is 24 participants, and 2 covariates were determined to be a reasonable limit. Analyses were performed using SAS 9.3 (SAS Institute) or Stata 13.1 (StataCorp LP). $P < 0.05$ was established as the level of statistical significance.

Results

Study Participants, Entire Cohort

Fifty patients consented to study participation prior to baseline coronary angiography. Two patients who underwent initial cardiac catheterization developed severe vasospasm during 10^{-6} mol/L acetylcholine infusion. They were successfully treated during the procedure and did well clinically but did not participate further in this trial or undergo randomization. Another 19 patients did not meet angiographic inclusion criteria and were considered screen failures. Consequently, 29 patients were enrolled in the study and underwent

randomization. A total of 25 patients returned for follow-up; 1 case was excluded from analysis due to poor data quality (Figure 1).

For the remaining 24 patients, physiological interrogation was performed in the left circumflex artery for 1 patient and in the left anterior descending artery for 23 patients. Table 1 displays baseline patient characteristics. At follow-up, both

Table 1. Patient Demographics and Characteristics

	Total (n=24)	Atenolol (n=12)	Nebivolol (n=12)	P Value
Age, y	52.5±10.3	49.8±10.7	55.2±9.5	0.21
Male	9 (38)	5 (42)	4 (33)	0.67
White race	18 (75)	8 (67)	10 (83)	0.35
Body mass index	29.1±5.8	30.0±6.4	28.2±5.2	0.46
Follow-up time period, months	12.4±1.0	12.5±0.6	12.4±1.3	0.81
Cardiovascular risk factors				
Hypertension	16 (67)	9 (75)	7 (58)	0.39
Diabetes mellitus	4 (17)	2 (17)	2 (17)	1.00
Dyslipidemia	18 (75)	8 (67)	10 (83)	0.35
Prior myocardial infarction	4 (17)	2 (17)	2 (17)	1.00
Smoking history	12 (50)	7 (58)	5 (42)	0.41
Family history of coronary disease	11 (46)	4 (33)	7 (58)	0.22
Presentation				
Non-ST-segment elevation myocardial infarction	1 (4)	1 (8)	0 (0)	
Unstable angina	5 (21)	2 (17)	3 (25)	0.52
Stable angina	17 (71)	8 (67)	9 (75)	
Medication use				
Aspirin	20 (83)	10 (83)	10 (83)	1.00
P2Y ₁₂ inhibitor	6 (25)	3 (25)	3 (25)	1.00
Statin	23 (96)	12 (100)	11 (92)	0.31
Calcium channel blocker	11 (46)	7 (58)	4 (33)	0.22
Long-acting nitrate	17 (71)	10 (83)	7 (58)	0.18
ACE inhibitor or ARB	6 (25)	3 (25)	3 (25)	1.00

Values are expressed as n (%) or mean±SD. ACE indicates angiotensin-converting enzyme; ARB, angiotensin II receptor blocker.

systolic and diastolic blood pressures decreased numerically (*P* value not significant), but heart rate changed significantly by −5 beats per minute (interquartile range −11 to +1 beats per minute; *P*=0.02). Low-density lipoprotein cholesterol level also increased by 10 mg/dL (interquartile range −3 to +29 mg/dL; *P*=0.04). There were no significant changes in coronary physiology or endothelial function between baseline and follow-up (Table 2).

Baseline mean VH-IVUS run length was 58±17 mm, lumen area was 11.84±5.38 mm², EEM area was 17.08±7.35 mm², and plaque area was 5.24±4.07 mm². At follow-up, the change in EEM area was −0.33±2.31 mm² (*P*<0.0001), in lumen area was −0.51±2.54 mm² (*P*<0.0001), in plaque area was 0.18±2.21 mm² (*P*<0.0001), in fibrous area was −0.01±1.33 mm² (*P*=0.67), in fibrofatty area was −0.01±0.38 mm² (*P*=0.22), in necrotic core area was −0.02±0.64 mm² (*P*=0.07), and in dense calcium area was 0.03±0.21 mm² (*P*<0.0001).

Relationship Between Baseline Coronary WSS, Serial Arterial Remodeling, and Plaque Progression

Coronary WSS was calculated in 1843 VH-IVUS segments using computational fluid dynamics modeling. There were 428 (23%) low-, 920 (50%) intermediate-, and 495 (27%) high-WSS segments. At follow-up, low-WSS segments demonstrated an increase in plaque area (*P*<0.0001) and a decrease in lumen area (*P*<0.0001) compared with intermediate- and high-WSS segments (Table 3) and more constrictive remodeling (*P*=0.04) (Figure 4).

Comparisons Between Nebivolol and Atenolol

Between the 2 cohorts, there were no significant differences in clinical characteristics or cardiac medications (Table 1) or other baseline and follow-up variables such as cholesterol levels, inflammatory and oxidative stress biomarkers, coronary flow velocity reserve, hyperemic microvascular resistance, or coronary endothelial function (Table 2). There was a trend of more segments in the nebivolol cohort with low WSS (317 versus 111) and fewer segments with high WSS (175 versus 320) compared with the atenolol arm (Figure 5).

On VH-IVUS, nebivolol segments demonstrated significantly decreased EEM area (*P*=0.02) and lumen area (*P*=0.004) but similar changes in plaque components and number of TCFA per vessel compared with atenolol (Table 2). Nebivolol also showed increased plaque area at follow-up (*P*<0.001), whereas atenolol demonstrated plaque regression (*P*=0.047); however, the difference between the 2 arms was not significant (*P*=0.27). With respect to arterial remodeling, static remodeling (remodeling index) was similar between the

Table 2. Patient and Vessel Characteristics at Baseline and Change After 1 Year

	Baseline			Change After 1 Year		
	Atenolol (n=12)	Nebivolol (n=12)	P Value	Atenolol (n=12)	Nebivolol (n=12)	P Value
Vital signs						
Systolic BP, mm Hg	137 [122, 145]	143 [122, 159]	0.51	−8 [−25, 10]	−7 [−20, 1]	0.95
Diastolic BP, mm Hg	73 [71, 85]	78 [69, 92]	0.63	0 [−8, 14]	−8 [−14, 6]	0.08
Heart rate, bpm	71 [60, 85]	68 [62, 78]	0.91	−5 [−11, 6]	−6 [−11, −1]*	0.66
Fasting lipid panel						
Total cholesterol, mg/dL	158 [136, 171]	149 [119, 160]	0.13	15 [−1, 31]	14 [−2, 55]	0.80
HDL cholesterol, mg/dL	48 [38, 54]	44 [43, 54]	0.75	3 [−5, 16]	−3 [−8, 2]	0.16
LDL cholesterol, mg/dL	87 [69, 104]	81 [72, 115]	0.52	6 [−3, 29]	13 [−4, 35]	0.89
Markers of inflammation and oxidative stress						
C-reactive protein, mg/L	1.87 [0.50, 3.82]	2.05 [1.30, 4.06]	0.48	0.33 [−1.72, 2.48]	0.07 [−0.78, 0.42]	0.72
Cystine, μ mol/L	84 [72, 112]	88 [79, 108]	0.41	10 [−4, 20]	17 [−7, 43]	0.37
Glutathione, μ mol/L	1.04 [0.87, 1.60]	0.98 [0.79, 1.26]	0.74	−0.13 [−0.56, 0.46]	−0.01 [−0.04, 0.17]	0.52
Cystine/glutathione ratio	84 [63, 100]	88 [69, 139]	0.53	31 [−2, 44]	15 [−24, 48]	0.78
Physiology, endothelial function, and vessel characteristics						
FFR	0.98 [0.94, 1.00]	0.91 [0.90, 0.98]	0.08	−0.02 [−0.08, 0.01]	−0.01 [−0.03, 0.05]	0.39
CFR	2.07 [1.82, 2.38]	1.87 [1.62, 2.33]	0.74	0.41 [0.06, 0.48]	0.71 [−0.58, 1.26]	0.97
HMR	1.75 [1.47, 2.66]	1.91 [1.46, 2.21]	0.89	0.07 [−0.54, 1.07]	−0.06 [−0.24, 0.43]	1.00
%Diameter change to ACh	−5 [−22, 3]	−2 [−8, 15]	0.47	2 [−11, 30]	3 [−12, 25]	0.89
%CBF change to ACh	60 [−11, 225]	142 [37, 181]	0.81	−5 [−172, 121]	87 [30, 385]	0.47
TCFAs per patient	2.2 \pm 1.2	1.6 \pm 1.0	0.27	−0.4 \pm 0.8	−0.3 \pm 1.0	0.94
Segment characteristics						
VH-IVUS run length, mm	54.3 \pm 10.9	62.5 \pm 21.1	0.25			
Minimum lumen area, mm ²	6.11 [3.85, 7.15]	4.15 [3.87, 7.77]	0.93			
Static remodeling	0.60 \pm 0.19	0.58 \pm 0.22	0.50			
EEM area, mm ²	16.5 \pm 7.3	17.5 \pm 7.3	0.76	0.20 \pm 1.99*	−0.78 \pm 2.46*	0.02
Lumen area, mm ²	10.9 \pm 4.5	12.7 \pm 5.9	0.41	0.33 \pm 2.08*	−1.22 \pm 2.68*	0.004
Plaque area, mm ²	5.7 \pm 4.8	4.9 \pm 3.3	0.66	−0.13 \pm 2.44*	0.44 \pm 1.95*	0.27
FI area, mm ²	1.67 \pm 2.86	1.08 \pm 1.66	0.51	−0.16 \pm 1.58*	0.14 \pm 1.02*	0.26
FF area, mm ²	0.23 \pm 0.46	0.16 \pm 0.35	0.57	−0.04 \pm 0.38*	0.02 \pm 0.38*	0.27
NC area, mm ²	0.48 \pm 1.07	0.36 \pm 0.80	0.77	−0.07 \pm 0.76*	0.03 \pm 0.49*	0.35
DC area, mm ²	0.09 \pm 0.17	0.15 \pm 0.38	0.28	0.01 \pm 0.17*	0.04 \pm 0.24*	0.34

Values are expressed as mean \pm SD or median [IQR]. ACh indicates acetylcholine; BP, blood pressure; bpm, beats per minute; CBF, coronary blood flow; CFR, coronary flow reserve; DC indicates dense calcium; EEM, external elastic membrane; FF, fibrofatty; FFR, fractional flow reserve; FI, fibrous; HDL, high-density lipoprotein; HMR, hyperemic myocardial resistance; LDL, low-density lipoprotein; NC, necrotic core; RI, remodeling index; TCFAs, thin-capped fibroatheromas; VH-IVUS, virtual histology intravascular ultrasound.

*Significant change from baseline ($P<0.05$).

2 groups, but serial remodeling was significantly different ($P=0.002$), with nebivolol segments demonstrating more constrictive remodeling (73% versus 46%) and less excessive expansive remodeling (16% versus 39%) than atenolol (Figure 6).

These observations could have been related to differences in baseline WSS patterns between the arms or to pharmaco-

logical therapy with the 2 different β -blockers, so VH-IVUS results were stratified by categories of WSS (Table 4) and β -blocker (Table 5). Among low-WSS segments (Table 4), those treated with nebivolol demonstrated decreased Δ EEM area compared with atenolol ($P=0.02$), consistent with a higher percentage of constrictive serial remodeling (83% versus 63%).

Table 3. Comparison of the Change in Virtual Histology Intravascular Ultrasound Measures After 1 year by Baseline WSS Category

Characteristic	Low WSS (n=428)	Intermediate WSS (n=920)	High WSS (n=495)	P Value
ΔLumen area, mm ²	-1.17±1.24	-0.64±1.61	0.61±2.15	<0.0001
ΔEEM area, mm ²	-0.70±1.32	-0.37±1.29	0.05±1.82	0.40
ΔPlaque area, mm ²	0.47±1.37	0.27±1.82	-0.56±2.77	<0.0001
ΔFibrous area, mm ²	0.21±0.76	0.02±1.08	-0.47±1.64	<0.0001
ΔFibrofatty area, mm ²	0.04±0.30	-0.01±0.24	-0.05±0.35	<0.0001
ΔNecrotic core area, mm ²	-0.07±0.71	-0.01±0.66	-0.17±0.88	<0.0001
ΔDense calcium area, mm ²	-0.01±0.22	0.04±0.22	0.04±0.26	<0.0001

Values are expressed as mean±SD. EEM indicates external elastic membrane; WSS, wall shear stress.

Table 5 compares VH-IVUS changes by WSS categories within each β -blocker cohort. Compared with high-WSS segments, low-WSS segments demonstrated greater decrease in lumen area ($P<0.0001$) and increase in plaque area ($P<0.01$). After adjustment for β -blocker, WSS category remained an independent predictor of changes in lumen area ($P<0.0001$) and plaque area ($P<0.0001$).

Discussion

This investigation is the first randomized controlled clinical trial studying the impact of a β_1 -blocker with endothelial β_3 -receptor agonist activity on the proatherosclerotic effect of coronary WSS. The major observations were as follows: First, there was greater plaque progression ($P<0.0001$) and constrictive remodeling in segments with low WSS ($P=0.04$) and, conversely, greater plaque regression and excessive expansive remodeling in segments with high WSS. Second,

there were greater reductions in lumen area ($P=0.004$) and vessel area ($P=0.02$), resulting in more constrictive remodeling, with nebivolol ($P=0.002$), likely driven by a trend toward more low-WSS segments in the nebivolol cohort ($P=0.06$). Third, after adjusting for the type of β -blocker therapy, low-WSS segments remained significantly associated with lumen loss and plaque progression ($P<0.0001$). Fourth, there were no significant differences in oxidative stress or inflammatory biomarker levels, endothelial function, microvascular function, or number of TCFA per vessel between nebivolol and atenolol.

Coronary atherosclerosis pathophysiology operates through complex multitude of pathways, including endothelial dysfunction as a conduit for systemic risk factors to affect the vasculature.^{18,26,27} The considerable number of investigations into the effects of WSS magnitudes on plaque development emphasizes this complexity. Low WSS can promote atherogenesis by changing endothelial cell morphology,² enhancing

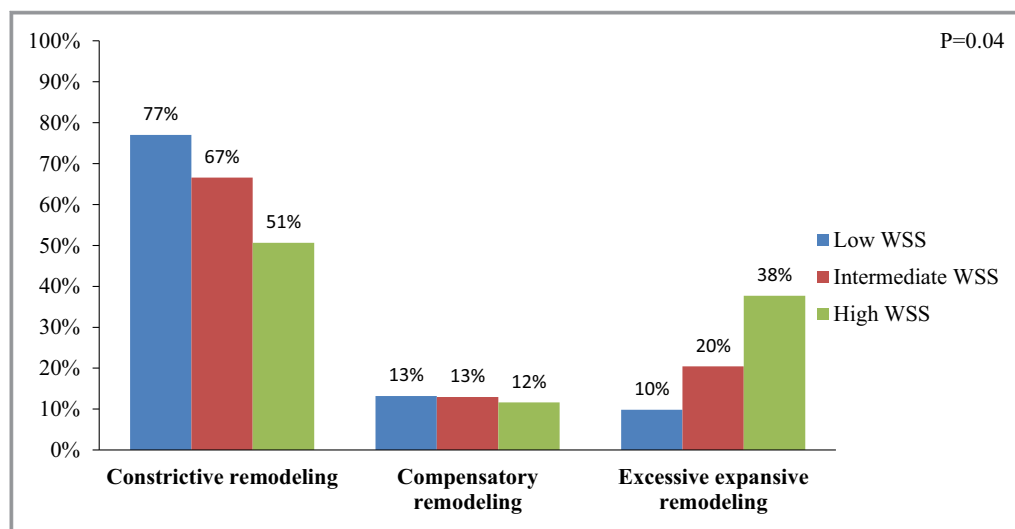


Figure 4. Serial arterial remodeling by baseline WSS categories at 1 year follow up. P value is for comparison of frequency of 3 remodeling groups across 3 WSS categories. WSS indicate wall shear stress.

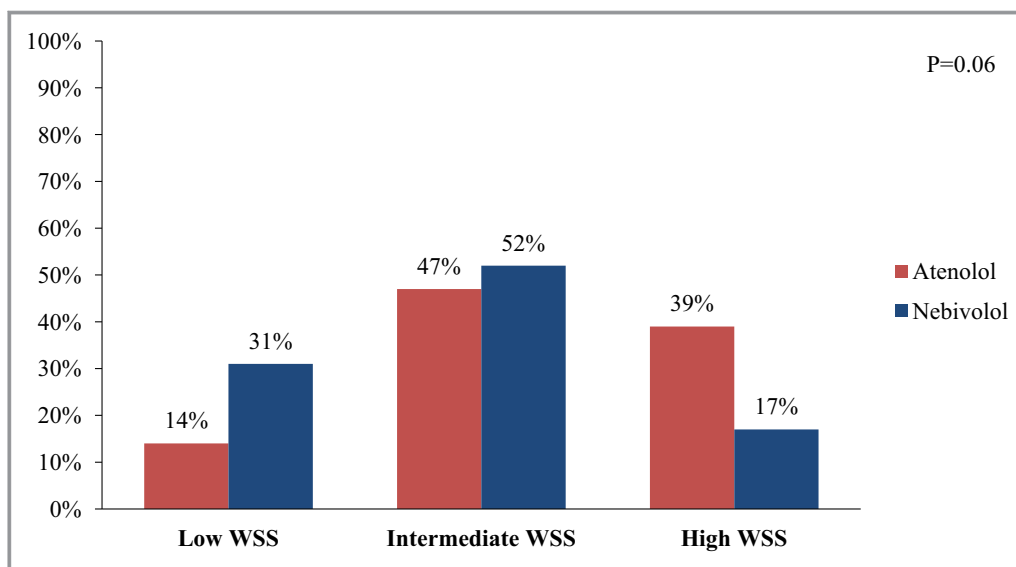


Figure 5. Distribution of baseline WSS by β -blocker. *P* value is for comparison of the frequency of 3 WSS categories across 2 β -blockers. WSS indicates wall shear stress.

production of reactive oxygen species and inflammatory molecules,²² and stimulating vascular smooth muscle cell migration.^{8,28} In our study, we observed that low-WSS regions were associated with more constrictive remodeling (Δ EEM -0.70 mm², $P=0.04$) and an absolute increase in plaque area of 0.47 mm² ($P<0.0001$). Conversely, high WSS can also contribute to plaque destabilization.^{4,10,29–31} Histological studies have implicated high WSS in smooth muscle cell apoptosis and proteoglycan matrix degradation,²⁹ whereas animal studies have demonstrated increased mechanical strain, vascular inflammation, macrophage activity, and expansive remodeling in high-WSS regions.^{30,32} We previously observed in human coronary arteries that, compared with intermediate-WSS segments, high-WSS segments trended toward more excessive expansive arterial remodeling,^{9,23} an exaggerated remodeling pattern in which both vessel and lumen dimensions increase proportionally more than plaque area. Although this type of remodeling in high-WSS segments may be partially explained by adaptive arterial enlargement in an attempt to restore WSS to a more physiological level,³¹ it can also drive plaque progression through continued lipid accumulation and inflammation. In this study, we demonstrated again that high-WSS regions were compensated by excessive expansive remodeling (Figure 5) with fibrous and fibrofatty tissue regression (Table 3).

The observation that nebivolol patients had more constrictive remodeling and lumen loss compared with atenolol patients in this study was interesting. Although this was a double-blinded randomized controlled trial, the nebivolol cohort had a numerically greater number of low coronary WSS segments per patient compared with the atenolol cohort (26.4 versus 9.3, $P=0.06$), despite having similar baseline

plaque areas (4.9 mm² versus 5.7 mm², $P=0.66$), static vascular remodeling (remodeling index 0.58 versus 0.60 , $P=0.50$), and coronary flow reserve (1.87 versus 2.07 , $P=0.74$). After adjusting for type of β -blocker, low WSS remained significantly associated with plaque progression and lumen loss (both $P<0.0001$), suggesting that WSS and not type of β -blocker therapy was driving these findings.

Interestingly, in our study, nebivolol and atenolol had similar changes in lipid profiles, inflammation and oxidative stress biomarkers, and coronary endothelial and microvascular function. In another study of hypertensive patients, we also observed no differences between nebivolol and metoprolol regarding pulse wave velocity, a noninvasive measurement of arterial stiffness and endothelial function, or oxidative stress biomarker levels.³³ In addition, there were no significant differences between nebivolol and atenolol with respect to necrotic core area or the number of TCFA per vessel. Taken together, the current investigation demonstrates no significant favorable or adverse effects of nebivolol compared with atenolol on comprehensive atherosclerosis phenotyping.

Despite the multidimensional nature of atherosclerosis pathophysiology, previous mechanistic investigations into the impact of pharmacotherapies on atherosclerosis development have generally relied on basic measures of plaque assessment such as the change in carotid intima media thickness^{34,35} or coronary atheroma volume.^{36–38} These measures may underestimate the effect of antiatherosclerotic therapies on the multiple known atherosclerotic pathways and processes. To our knowledge, no prior investigation has comprehensively examined the incremental effect of a potential antiatherosclerotic therapy on epicardial and microvascular endothelial-dependent and -independent function, atherosclerosis burden and com-

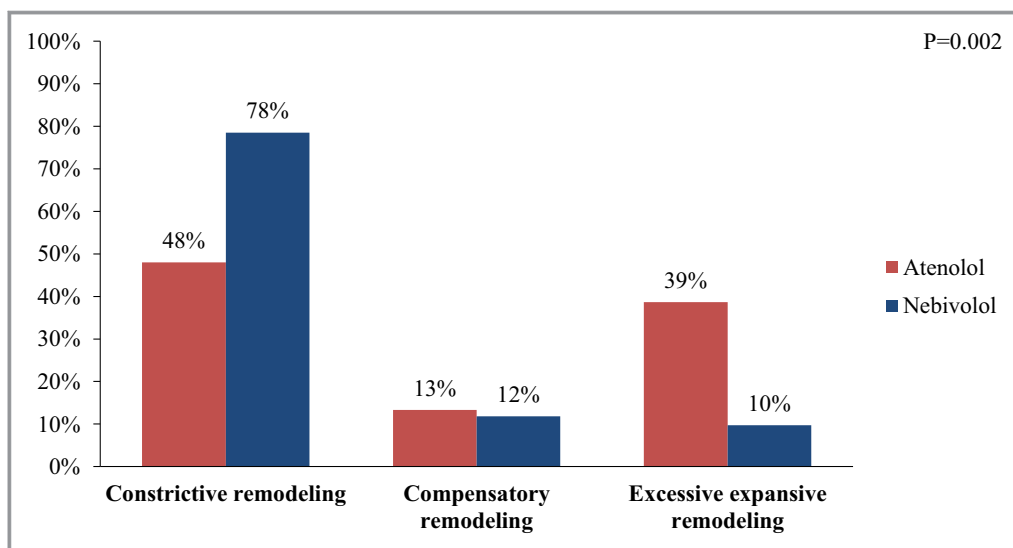


Figure 6. Serial arterial remodeling by β -blocker at 1-year follow-up. *P* value is for comparison of the frequency of 3 remodeling groups across 2 β -blocker categories.

position, static and serial arterial remodeling, and oxidative stress and inflammatory pathways in the context of coronary WSS. This investigation offers a blueprint for how novel cardiovascular therapies can be evaluated, given the numerous possible mechanisms for therapeutic intervention.

Limitations

The study was powered for VH-IVUS end points but may not have been adequately powered to detect changes in endothelial and microvascular function or number of TCFA per artery. Although the nebivolol dose used in this trial was approved for clinical use, the effective concentration may be too low or the

duration of follow-up insufficient to affect the prespecified end points. Nevertheless, this study is the most comprehensive atherosclerosis phenotyping double-blinded randomized controlled trial performed thus far and can establish the methodology for future coronary atherosclerosis trials for novel pharmaceutical agents such as protein convertase subtilisin/kexin type 9 inhibitors.

Plaque composition data are derived from VH-IVUS, which has inherent limitations compared with histology but can be performed in vivo in coronary arteries and has been validated by several studies.^{6–9,20,21} In addition, although there were many arterial segments, the effective sample size was 24 participants; this limits the number of covariates used in

Table 4. Comparison of Change in Virtual Histology Intravascular Ultrasound Measures by β -Blocker, Stratified by Baseline Wall Shear Stress Categories

	Low WSS			Intermediate WSS			High WSS		
	Atenolol (n=111)	Nebivolol (n=317)	<i>P</i> Value	Atenolol (n=382)	Nebivolol (n=538)	<i>P</i> Value	Atenolol (n=320)	Nebivolol (n=175)	<i>P</i> Value
Δ Lumen area, mm ²	-0.80±1.15	-1.29±1.25	0.22	0.21±1.79	-1.24±1.15	0.002	1.15±2.38	-0.39±1.08	0.02
Δ EEM area, mm ²	0.01±1.06	-0.95±1.31	0.02	-0.02±1.53	-0.62±1.02	0.15	0.29±1.96	-0.40±1.44	0.43
Δ Plaque area, mm ²	0.81±1.05	0.35±1.45	0.30	-0.23±2.38	0.62±1.15	0.28	-0.86±3.23	-0.01±1.45	0.30
Δ FI area, mm ²	0.36±0.84	0.16±0.72	0.23	-0.18±1.44	0.16±0.68	0.40	-0.66±1.94	-0.13±0.79	0.31
Δ FF area, mm ²	0.04±0.23	0.03±0.32	0.47	-0.03±0.25	0.00±0.24	0.77	-0.09±0.38	0.01±0.27	0.34
Δ NC area, mm ²	0.07±0.34	-0.12±0.79	0.45	-0.15±0.92	0.09±0.35	0.14	-0.25±1.06	-0.01±0.30	0.25
Δ DC area, mm ²	-0.01±0.12	-0.01±0.24	0.78	0.01±0.16	0.06±0.25	0.19	0.02±0.22	0.09±0.31	0.15

P-values are for comparison between 2 β -blocker categories. DC indicates dense calcium; EEM, external elastic membrane; FF, fibrofatty; FI, fibrous; NC, necrotic core; WSS, wall shear stress.

Table 5. Comparison of Change in VH-IVUS Measures by Baseline WSS Categories, Stratified by Type of β -Blocker

	Atenolol				Nebivolol			
	Low WSS (n=111)	Intermediate WSS (n=382)	High WSS (n=320)	P Value	Low WSS (n=317)	Intermediate WSS (n=538)	High WSS (n=175)	P Value
Δ Lumen area, mm ²	-0.80±1.15	0.21±1.79	1.15±2.38	<0.0001	-1.29±1.25	-1.24±1.15	-0.39±1.08	<0.0001
Δ Vessel area, mm ²	0.01±1.06	-0.02±1.53	0.29±1.96	0.002	-0.95±1.31	-0.62±1.02	-0.40±1.44	<0.0001
Δ Plaque area, mm ²	0.81±1.05	-0.23±2.38	-0.86±3.23	<0.0001	0.35±1.45	0.62±1.15	-0.01±1.45	0.006
Δ FI area, mm ²	0.36±0.84	-0.18±1.44	-0.66±1.94	<0.0001	0.16±0.72	0.16±0.68	-0.13±0.79	<0.0001
Δ FF area, mm ²	0.04±0.23	-0.03±0.25	-0.09±0.38	<0.0001	0.03±0.32	0.00±0.24	0.01±0.27	0.02
Δ NC area, mm ²	0.07±0.34	-0.15±0.92	-0.25±1.06	<0.0001	-0.12±0.79	0.09±0.35	-0.01±0.30	0.01
Δ DC area, mm ²	-0.01±0.12	0.01±0.16	0.02±0.22	0.57	-0.01±0.24	0.06±0.25	0.09±0.31	<0.0001

P-values are for comparison among 3 WSS categories. DC indicates dense calcium; FF, fibro-fatty; FI, fibrous; NC, necrotic core; WSS, wall shear stress.

multivariate analysis. Finally, this was a randomized clinical trial between nebivolol and atenolol; however, the constrictive remodeling seen in the nebivolol arm is likely related to the greater number of baseline segments with low WSS. Although randomization can be readily performed with prespecified balance in demographics, it is currently impractical, given the time- and resource-intensive nature of computational fluid dynamic modeling, to randomize patients based on their distribution of coronary WSS segments.

Conclusions

Compared with atenolol, nebivolol demonstrated greater luminal reduction and constrictive remodeling, but this was likely driven by the higher number of low-WSS segments in the nebivolol cohort. There were no significant differences in coronary endothelial function or microvascular function between treatment groups. This study suggests that any impact of an endothelial β_3 -receptor agonist on the effects of WSS magnitudes or on the natural history of epicardial and microvascular atherosclerosis, if present, is minimal. Importantly, it lays down the methodological framework for future mechanistic evaluation of pharmacotherapy on human coronary atherosclerosis.

Acknowledgments

We thank the Emory University Clinical Biomarkers Lab for analyzing the oxidative stress biomarker samples and the Emory University Hospital cardiac catheterization laboratory support staff for their help in the procedures.

Sources of Funding

Forest Laboratories financed this study. The NIH Ruth L. Kirschstein National Research Service Awards training grant (5T32HL007745) supported Hung and Eshtehardi. The American Heart Association Postdoctoral Fellowships supported Molony and Timmins.

Disclosures

McDaniel consults for Medtronic, Inc. Samady receives research funding from Forest Laboratories an Allergan Affiliate, Volcano Corporation, St. Jude Medical, Gilead Sciences, Medtronic, Inc and Abbott Vascular.

References

- Krams R, Wentzel JJ, Oomen JA, Vinke R, Schuurbijs JC, de Feyter PJ, Serruys PW, Slager CJ. Evaluation of endothelial shear stress and 3D geometry as factors determining the development of atherosclerosis and remodeling in human coronary arteries in vivo. Combining 3D reconstruction from angiography and IVUS (ANGUS) with computational fluid dynamics. *Arterioscler Thromb Vasc Biol.* 1997;17:2061–2065.
- Levesque MJ, Liepsch D, Moravec S, Nerem RM. Correlation of endothelial cell shape and wall shear stress in a stenosed dog aorta. *Arteriosclerosis.* 1986;6:220–229.
- Eshtehardi P, McDaniel MC, Suo J, Dhawan SS, Timmins LH, Binongo JN, Golub LJ, Corban MT, Finn AV, Oshinski JN, Quyyumi AA, Giddens DP, Samady H. Association of coronary wall shear stress with atherosclerotic plaque burden, composition, and distribution in patients with coronary artery disease. *J Am Heart Assoc.* 2012;1:e002543 doi: 10.1161/JAHA.112.002543.
- Fukumoto Y, Hiro T, Fujii T, Hashimoto G, Fujimura T, Yamada J, Okamura T, Matsuzaki M. Localized elevation of shear stress is related to coronary plaque rupture: a 3-dimensional intravascular ultrasound study with in-vivo color mapping of shear stress distribution. *J Am Coll Cardiol.* 2008;51:645–650.
- Koskinas KC, Feldman CL, Chatzizisis YS, Coskun AU, Jonas M, Maynard C, Baker AB, Papafaklis MI, Edelman ER, Stone PH. Natural history of experimental coronary atherosclerosis and vascular remodeling in relation to endothelial shear stress: a serial, in vivo intravascular ultrasound study. *Circulation.* 2010;121:2092–2101.
- Stone PH, Coskun AU, Kinlay S, Clark ME, Sonka M, Wahle A, Ilegbusi OJ, Yeghiazarians Y, Popma JJ, Orav J, Kuntz RE, Feldman CL. Effect of endothelial shear stress on the progression of coronary artery disease, vascular remodeling, and in-stent restenosis in humans: in vivo 6-month follow-up study. *Circulation.* 2003;108:438–444.
- Stone PH, Coskun AU, Kinlay S, Popma JJ, Sonka M, Wahle A, Yeghiazarians Y, Maynard C, Kuntz RE, Feldman CL. Regions of low endothelial shear stress are the sites where coronary plaque progresses and vascular remodeling occurs in humans: an in vivo serial study. *Eur Heart J.* 2007;28:705–710.
- Stone PH, Saito S, Takahashi S, Makita Y, Nakamura S, Kawasaki T, Takahashi A, Katsuki T, Nakamura S, Namiki A, Hirohata A, Matsumura T, Yamazaki S, Yokoi H, Tanaka S, Otsuji S, Yoshimachi F, Honye J, Harwood D, Reitman M, Coskun AU, Papafaklis MI, Feldman CL, Investigators P. Prediction of progression of coronary artery disease and clinical outcomes using vascular profiling of endothelial shear stress and arterial plaque characteristics: the PREDICTION Study. *Circulation.* 2012;126:172–181.
- Samady H, Eshtehardi P, McDaniel MC, Suo J, Dhawan SS, Maynard C, Timmins LH, Quyyumi AA, Giddens DP. Coronary artery wall shear stress is

- associated with progression and transformation of atherosclerotic plaque and arterial remodeling in patients with coronary artery disease. *Circulation*. 2011;124:779–788.
10. Wentzel JJ, Schuurbiens JC, Gonzalo Lopez N, Gijssen FJ, van der Giessen AG, Groen HC, Dijkstra J, Garcia-Garcia HM, Serruys PW. In vivo assessment of the relationship between shear stress and necrotic core in early and advanced coronary artery disease. *EuroIntervention*. 2013;9:989–995; discussion 995.
 11. Chatzizisis YS, Jonas M, Beigel R, Coskun AU, Baker AB, Stone BV, Maynard C, Gerrity RG, Daley W, Edelman ER, Feldman CL, Stone PH. Attenuation of inflammation and expansive remodeling by Valsartan alone or in combination with Simvastatin in high-risk coronary atherosclerotic plaques. *Atherosclerosis*. 2009;203:387–394.
 12. Sorrentino SA, Doerries C, Manes C, Speer T, Dessy C, Lobysheva I, Mohmand W, Akbar R, Bahlmann F, Besler C, Schaefer A, Hilfiker-Kleiner D, Luscher TF, Balligand JL, Drexler H, Landmesser U. Nebivolol exerts beneficial effects on endothelial function, early endothelial progenitor cells, myocardial neovascularization, and left ventricular dysfunction early after myocardial infarction beyond conventional beta1-blockade. *J Am Coll Cardiol*. 2011;57:601–611.
 13. Arosio E, De Marchi S, Prior M, Zannoni M, Lechi A. Effects of nebivolol and atenolol on small arteries and microcirculatory endothelium-dependent dilation in hypertensive patients undergoing isometric stress. *J Hypertens*. 2002;20:1793–1797.
 14. Dessy C, Saliez J, Ghisdal P, Daneau G, Lobysheva I, Frerart F, Belge C, Jnaoui K, Noirhomme P, Feron O, Balligand JL. Endothelial beta3-adrenoreceptors mediate nitric oxide-dependent vasorelaxation of coronary microvessels in response to the third-generation beta-blocker nebivolol. *Circulation*. 2005;112:1198–1205.
 15. Tzemos N, Lim PO, MacDonald TM. Nebivolol reverses endothelial dysfunction in essential hypertension: a randomized, double-blind, crossover study. *Circulation*. 2001;104:511–514.
 16. Erdogan D, Gullu H, Caliskan M, Ciftci O, Baycan S, Yildirim A, Muderrisoglu H. Nebivolol improves coronary flow reserve in patients with idiopathic dilated cardiomyopathy. *Heart*. 2007;93:319–324.
 17. Fogari R, Zoppi A, Lazzari P, Mugellini A, Lusardi P, Preti P, Van Nueten L, Vertommen C. Comparative effects of nebivolol and atenolol on blood pressure and insulin sensitivity in hypertensive subjects with type II diabetes. *J Hum Hypertens*. 1997;11:753–757.
 18. Dhawan SS, Eshtehardi P, McDaniel MC, Fike LV, Jones DP, Quyyumi AA, Samady H. The role of plasma aminothiois in the prediction of coronary microvascular dysfunction and plaque vulnerability. *Atherosclerosis*. 2011;219:266–272.
 19. Mintz GS, Nissen SE, Anderson WD, Bailey SR, Erbel R, Fitzgerald PJ, Pinto FJ, Rosenfield K, Siegel RJ, Tuzcu EM, Yock PG. American College of Cardiology Clinical Expert Consensus Document on Standards for Acquisition, Measurement and Reporting of Intravascular Ultrasound Studies (IVUS). A report of the American College of Cardiology Task Force on Clinical Expert Consensus Documents. *J Am Coll Cardiol*. 2001;37:1478–1492.
 20. Garcia-Garcia HM, Mintz GS, Lerman A, Vince DG, Margolis MP, van Es GA, Morel MAM, Nair A, Virmani R, Burke AP, Stone GW, Serruys PW. Tissue characterisation using intravascular radiofrequency data analysis: recommendations for acquisition, analysis, interpretation and reporting. *EuroIntervention*. 2009;5:177–189.
 21. Nasu K, Tsuchikane E, Katoh O, Vince DG, Virmani R, Surmely JF, Murata A, Takeda Y, Ito T, Ehara M, Matsubara T, Terashima M, Suzuki T. Accuracy of in vivo coronary plaque morphology assessment: a validation study of in vivo virtual histology compared with in vitro histopathology. *J Am Coll Cardiol*. 2006;47:2405–2412.
 22. Chatzizisis YS, Baker AB, Sukhova GK, Koskinas KC, Papafakis MI, Beigel R, Jonas M, Coskun AU, Stone BV, Maynard C, Shi GP, Libby P, Feldman CL, Edelman ER, Stone PH. Augmented expression and activity of extracellular matrix-degrading enzymes in regions of low endothelial shear stress colocalize with coronary atheromata with thin fibrous caps in pigs. *Circulation*. 2011;123:621–630.
 23. Corban MT, Eshtehardi P, Suo J, McDaniel MC, Timmins LH, Rassoul-Arzrumly E, Maynard C, Mekonnen G, King S III, Quyyumi AA, Giddens DP, Samady H. Combination of plaque burden, wall shear stress, and plaque phenotype has incremental value for prediction of coronary atherosclerotic plaque progression and vulnerability. *Atherosclerosis*. 2014;232:271–276.
 24. Rogers WH. Regression standard errors in clustered samples. *Stata Tech Bull*. 1993;13:19–23.
 25. Williams RL. A note on robust variance estimation for cluster-correlated data. *Biometrics*. 2000;56:645–646.
 26. Treasure CB, Klein JL, Weintraub WS, Talley JD, Stillabower ME, Kosinski AS, Zhang J, Boccuzzi SJ, Cedarholm JC, Alexander RW. Beneficial effects of cholesterol-lowering therapy on the coronary endothelium in patients with coronary artery disease. *N Engl J Med*. 1995;332:481–487.
 27. Halcox JP, Schenke WH, Zalos G, Mincemoyer R, Prasad A, Waclawiw MA, Nour KR, Quyyumi AA. Prognostic value of coronary vascular endothelial dysfunction. *Circulation*. 2002;106:653–658.
 28. Liu SQ, Goldman J. Role of blood shear stress in the regulation of vascular smooth muscle cell migration. *IEEE Trans Biomed Eng*. 2001;48:474–483.
 29. Mattsson EJ, Kohler TR, Vergel SM, Clowes AW. Increased blood flow induces regression of intimal hyperplasia. *Arterioscler Thromb Vasc Biol*. 1997;17:2245–2249.
 30. Castier Y, Brandes RP, Leseche G, Tedgui A, Lehoux S. p47phox-dependent NADPH oxidase regulates flow-induced vascular remodeling. *Circ Res*. 2005;97:533–540.
 31. Dolan JM, Kolega J, Meng H. High wall shear stress and spatial gradients in vascular pathology: a review. *Ann Biomed Eng*. 2013;41:1411–1427.
 32. Tronc F, Mallat Z, Lehoux S, Wassef M, Esposito B, Tedgui A. Role of matrix metalloproteinases in blood flow-induced arterial enlargement: interaction with NO. *Arterioscler Thromb Vasc Biol*. 2000;20:E120–E126.
 33. Hayek SS, Poole JC, Neuman R, Morris AA, Khayata M, Kavtaradze N, Topel ML, Binongo JG, Li Q, Jones DP, Waller EK, Quyyumi AA. Differential effects of nebivolol and metoprolol on arterial stiffness, circulating progenitor cells, and oxidative stress. *J Am Soc Hypertens*. 2015;9:206–213.
 34. Howard BV, Roman MJ, Devereux RB, Fleg JL, Galloway JM, Henderson JA, Howard WJ, Lee ET, Mete M, Poolaw B, Ratner RE, Russell M, Silverman A, Stylianou M, Umans JG, Wang W, Weir MR, Weissman NJ, Wilson C, Yeh F, Zhu J. Effect of lower targets for blood pressure and LDL cholesterol on atherosclerosis in diabetes: the SANDS randomized trial. *JAMA*. 2008;299:1678–1689.
 35. Nohara R, Daida H, Hata M, Kaku K, Kawamori R, Kishimoto J, Kurabayashi M, Masuda I, Sakuma I, Yamazaki T, Yokoi H, Yoshida M; Justification for Atherosclerosis Regression Treatment I. Effect of intensive lipid-lowering therapy with rosuvastatin on progression of carotid intima-media thickness in Japanese patients: Justification for Atherosclerosis Regression Treatment (JART) study. *Circ J*. 2012;76:221–229.
 36. Nissen SE, Nicholls SJ, Sipahi I, Libby P, Raichlen JS, Ballantyne CM, Davignon J, Erbel R, Fruchart JC, Tardif JC, Schoenhagen P, Crowe T, Cain V, Wolski K, Goormastic M, Tuzcu EM; Investigators A. Effect of very high-intensity statin therapy on regression of coronary atherosclerosis: the ASTEROID trial. *JAMA*. 2006;295:1556–1565.
 37. Hirohata A, Yamamoto K, Miyoshi T, Hatanaka K, Hirohata S, Yamawaki H, Komatsubara I, Murakami M, Hirose E, Sato S, Ohkawa K, Ishizawa M, Yamaji H, Kawamura H, Kusachi S, Murakami T, Hina K, Ohe T. Impact of olmesartan on progression of coronary atherosclerosis: a serial volumetric intravascular ultrasound analysis from the OLIVUS (impact of OLmesarten on progression of coronary atherosclerosis: evaluation by intravascular ultrasound) trial. *J Am Coll Cardiol*. 2010;55:976–982.
 38. Puri R, Libby P, Nissen SE, Wolski K, Ballantyne CM, Barter PJ, Chapman MJ, Erbel R, Raichlen JS, Uno K, Kataoka Y, Tuzcu EM, Nicholls SJ. Long-term effects of maximally intensive statin therapy on changes in coronary atheroma composition: insights from SATURN. *Eur Heart J Cardiovasc Imaging*. 2014;15:380–388.